



	<b>Experiment title:</b> Unravelling the Twist in Narwhal Tusk with Hierarchical X-Ray Scattering Tensor Tomography	<b>Experiment number:</b> SC-5369
<b>Beamline:</b> ID15A	<b>Date of experiment:</b> from: 03/05/2023 to: 08/05/2023	<b>Date of report:</b> 07/07/2023
<b>Shifts:</b> 15	<b>Local contact(s):</b> Stefano Checchia	<i>Received at ESRF:</i>
<b>Names and affiliations of applicants</b> (* indicates experimentalists): <b>Dr. Adrian Rodriguez Palomo*</b> , Interdisciplinary Nanoscience Centre, Aarhus University, Denmark <b>Peter Vibe*</b> , Interdisciplinary Nanoscience Centre, Aarhus University, Denmark <b>Malene Jacobsen*</b> , Interdisciplinary Nanoscience Centre, Aarhus University, Denmark <b>Dr. Henrik Birkedal</b> , Department of Chemistry, Aarhus University, Denmark <b>Dr. Dimitra Athanasiadou*</b> , Department of Physics, Chalmers University of Technology, Sweden <b>Dr. Marianne Liebi*</b> , Photon Science Division, Paul Scherrer Institute, Switzerland		

### Report:

The aim of the experiment was to study the orientation of the narwhal tusk's building blocks (i.e., mineralised collagen fibrils) in the macroscopic length scale. This experiment belongs to a larger study with the goal of studying the orientation of the tusk's building blocks at different length scales to reconstruct the overall hierarchical structure of the left-hand spiral tusk (experimental report from experiment SC-5257). We hypothesize that the orientational arrangement of collagen fibrils and biomineral nanocrystals is directly related to the spiral nature of the tusk and its mechanical properties. Thereby its determination is an essential piece of the spiral puzzle of narwhal tusks.

Two samples were extracted at different positions in the tusk and mounted on PMMA rods instead of metallic needles to prevent X-ray absorption at high tilt angles. The samples were further milled to the right dimensions and shape with an in-house automated lathe. A cylindrical piece of narwhal tusk extracted radially from the pulp chamber (sample ID108, diameter: 5 mm, length: 7 mm) and a sample consisting of the tusk tip (sample ID105, diameter: 6 mm, length: 10 mm) were measured in this experiment.

The experimental configuration for small-angle X-ray scattering tensor tomography (SASTT) consisted of motorised stages for vertical and horizontal translation mounted on top of an Eulerian cradle with rotation in the horizontal axis ( $\beta$ ) and a motorised goniometer on top of the translation stages with rotation movement around the vertical axis ( $\alpha$ ). Initially, a Maxipix detector was placed downstream to record the scattering signal at a sample-to-detector distance of 4944 mm. An in-vacuum flight tube was placed between the sample and the detector to minimise absorption and scattering from the air. A semitransparent beamstop was used to record the beam transmission during the experiment. Multiple issues related to detector stability, which affected the quality of the recorded signal, and the transmission of the semitransparent beamstop at the used energy (60.0 keV), impeded obtaining data with good enough quality for the purpose. Based on the advice of the beamline staff, we decided to change the detector configuration and X-ray beam parameters. During this process, the beamline staff was of immense help, providing all the necessary assistance and support. A Pilatus 3 X CdTe 2M detector at a sample-to-detector distance of 2434 mm was used in the definitive configuration, with which we obtained high-quality data at an excellent signal-to-noise ratio. A He-filled plastic flight tube and an opaque beamstop were placed between the sample and the detector.

During the experiment, a 40.5 keV X-ray beam was used to obtain low enough X-ray absorption while maximizing the desired  $q$ -range ( $10^{-2} - 10^0 \text{ \AA}^{-1}$ ) including the scattering signal of the biomineral particles and the diffraction signal of the collagen  $D$ -period. The beam was focused to  $76 \times 90 \text{ \mu m}$  in the vertical and horizontal directions respectively. Each sample was raster-scanned on the beam with equal steps of  $150 \text{ \mu m}$  and an exposure time of  $20 \text{ ms}$ , collecting a total of  $\sim 250$  2D projections per sample in a rotation range  $\alpha = 0^\circ - 180^\circ$  for tilt  $\beta = 0^\circ$  ( $\Delta\alpha = 5.5^\circ$ ), and  $\alpha = 0^\circ - 360^\circ$  for  $\beta \neq 0^\circ$  ( $\Delta\alpha = 8.2^\circ$ ). A total of 6 tilt angles were used from  $\beta = 0^\circ - 41^\circ$  ( $\Delta\beta = 8.2^\circ$ ). The scattering signal in each scanning point was radially and azimuthally integrated with the integration software MatFRAIA [1] using 16 equally spaced azimuthal segments. The integrated scattering data were further combined in the corresponding 2D projections at each measured sample position using the recorded motor positions using custom-made software. Additionally to the scattering experiments, full-field computed tomography experiments were done in both samples to obtain the X-ray transmission signal, needed for the final reciprocal space map reconstruction. This technique only allowed us to measure the 2D transmission projections at a tilt  $\beta = 0^\circ$ . The transmission projections at all combinations of  $\alpha/\beta$  were obtained by tomographically reconstructing the 3D volume and calculating the synthetic projection of such 3D object using the rotation matrix at each  $\alpha/\beta$  combination. The scattering and transmission of 2D projections were eventually overlapped and aligned using an iterative alignment method [2]. The reconstruction of the reciprocal space map (RSM) was carried out following a procedure reported by Nielsen et al., [3] based on that described by Liebi et al. [4, 5]. The robustness of the reconstruction was checked by visual comparison of 2D orientation, anisotropy, and degree of orientation between the measurements and simulated projections of the reconstructed data. The degree of orientation was calculated as the ratio between the isotropic tensor coefficient, and the full tensor [1].

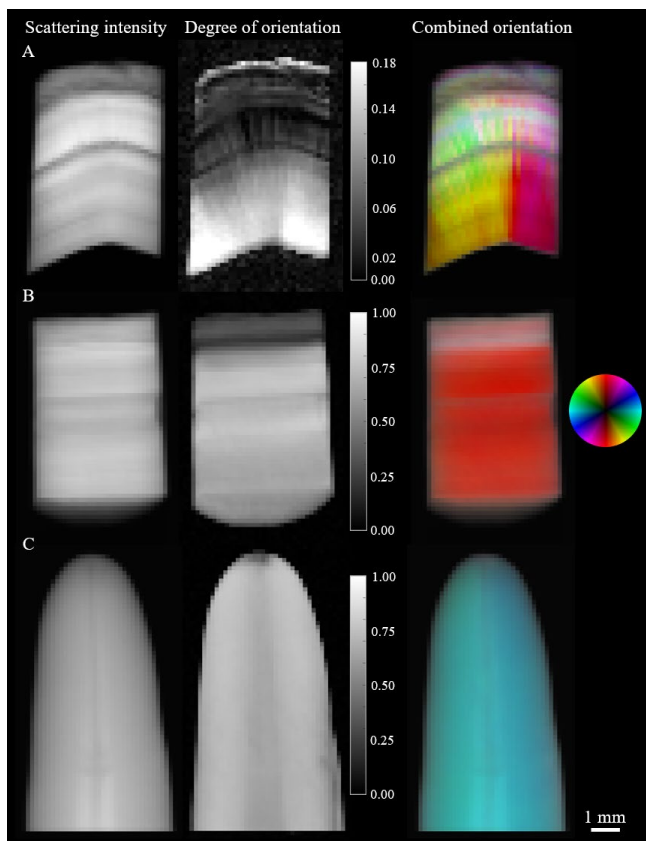


**Figure 1.** 2D projections of a  $q$ -range related to the mineral particles in samples ID108 in the transversal (A) and longitudinal (B) orientation ID105 (C). The combined orientation shows the main orientation of the scattering signal according to the colour wheel where the hue shows the angle, the saturation shows the asymmetric intensity and the value shows the symmetric intensity.

Currently, the scattering data has been integrated and the 2D projections built with the necessary metadata for the RSM reconstruction. The tomographic data has been reconstructed and the synthetic projections at all sample positions created together with the 2D scattering projections (Figure 1). The outer cementum layer (top area in Figures 1A and 1B) presents a lower degree of orientation compared to the dentine, which is highly aligned in the longitudinal direction as shown in Figure 1B. The tip of the tusk (Figure 1C) also shows a strong anisotropy in the longitudinal direction with a distinct variation between the left and right side, potentially from the helical macrostructure in the tusk. To further confirm that, the final 3D orientation reconstruction is needed.

The RSM reconstruction software has been updated to a new version with improved reconstruction quality and it is currently being adapted to the present data sets. A preliminary reconstruction of the reciprocal space map of the scattering signal corresponding to the mineral particles ( $q = 0.036 - 0.225 \text{ \AA}^{-1}$ ) was reconstructed with a cubic voxel size of  $150 \text{ \mu m}$  (Figure 2). The cementum layer has a lower degree of orientation in 3D as seen previously in the 2D slices. The 3D main orientation is predominantly longitudinal as shown by the cylinders in the 3D glyph (Figure 2A) with small deviations from the axial direction. In the next analysis step, a more robust reconstruction will be done for both samples, where the final macroscopic orientation model for the mineralised collagen fibres will be defined.

A manuscript is under preparation, which will contain the final results of this experiment after the analysis has been completed.

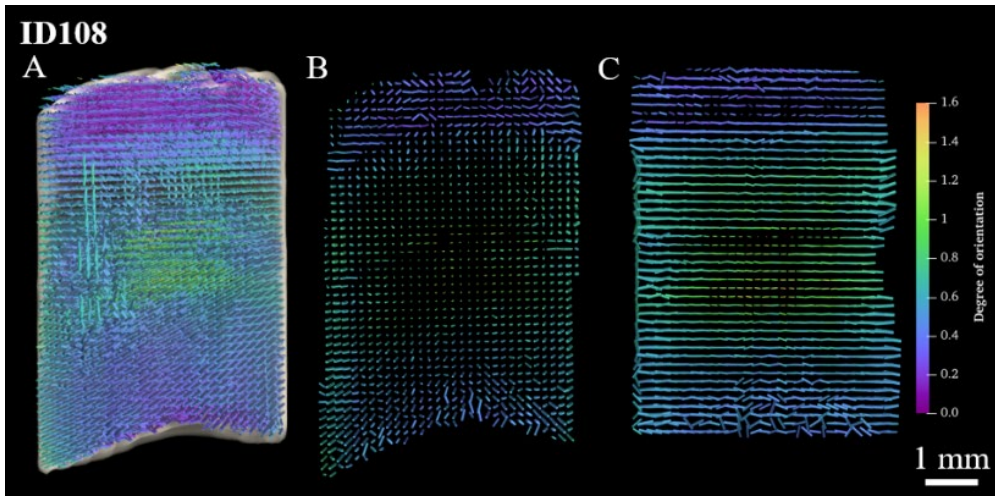


**Figure 2.** 3D representation of the mineralised collagen fibrils' main orientation in sample ID108. The transversal perspective of the 3D glyph (A) and two virtual slices in transversal (B) and longitudinal (C) orientations are shown with the cylinders representing the main orientation, the cylinder length the symmetric intensity and the colour the degree of orientation according to the colour scale.

### References:

- [1] A. Bernthz et al., *Journal of Synchrotron Radiation* 29 (6), 1420-1428 (2022).
- [2] M. Odstrčil et al., *Optics Express* 27 (25), 36637-36652 (2019).
- [3] L. C. Nielsen et al., arXiv:2305.07750v1 [cond-mat.mtrl-sci] (2023).
- [4] M. Liebi et al., *Nature* 527 (7578), 349-352 (2015).
- [5] M. Liebi, et al., *Acta Crystallographica A* 74 (1), 12-24 (2018).